Cell Research (2015) 25:1333-1351.

www.nature.com/cr

ORIGINAL ARTICLE

Tuberculosis is associated with expansion of a motile, permissive and immunomodulatory CD16$^+$ monocyte population via the IL-10/STAT3 axis

Claire Lastrucci[1, 2], Alan Bénard[1, 2, *], Luciana Balboa[3, *], Karine Pingris[1, 2], Shanti Souriant[1, 2], Renaud Poincloux[1, 2], Talal Al Saati[4], Voahangy Rasolofo[5], Pablo González-Montaner[6], Sandra Inwentarz[6], Eduardo Jose Moraña[6], Ivanela Kondova[7], Frank AW Verreck[7], Maria del Carmen Sasiain[3], Olivier Neyrolles[1, 2], Isabelle Maridonneau-Parini[1, 2], Geanncarlo Lugo-Villarino[1, 2, #], Céline Cougoule[1, 2, #]

[1]CNRS, Institut de Pharmacologie et de Biologie Structurale (IPBS), Département of Tuberculosis and Infection Biology, Toulouse, France; [2]Université de Toulouse; Université Paul Sabatier, UPS, IPBS, Toulouse, France; [3]Inmunologia de Enfermedades Respiratorias, Instituto de Medicina Experimental (IMEX)-CONICET, Academia Nacional de Medicina, Pacheco de Melo 3081, 1425, Buenos Aires, Argentina; [4]INSERM/UPS-US006/CREFRE, Service d'Histopathologie, CHU Purpan, 31024, Toulouse, France; [5]Mycobacteria Unit, Pasteur Institute in Antananarivo, Antananarivo, Madagascar; [6]Instituto Prof. Dr. Raúl Vaccarezza, Hospital de Infecciosas Dr. F.J. Muñiz, Buenos Aires, Argentina; [7]Department of Parasitology, Biomedical Primate Research Centre, Rijswijk, the Netherlands

The human CD14$^+$ monocyte compartment is composed by two subsets based on CD16 expression. We previously reported that this compartment is perturbed in tuberculosis (TB) patients, as reflected by the expansion of CD16$^+$ monocytes along with disease severity. Whether this unbalance is beneficial or detrimental to host defense remains to be elucidated. Here in the context of active TB, we demonstrate that human monocytes are predisposed to differentiate towards an anti-inflammatory (M2-like) macrophage activation program characterized by the CD16$^+$CD163$^+$MerTK$^+$pSTAT3$^+$ phenotype and functional properties such as enhanced protease-dependent motility, pathogen permissivity and immunomodulation. This process is dependent on STAT3 activation, and loss-of-function experiments point towards a detrimental role in host defense against TB. Importantly, we provide a critical correlation between the abundance of the CD16$^+$CD163$^+$MerTK$^+$pSTAT3$^+$ cells and the progression of the disease either at the local level in a non-human primate tuberculous granuloma context, or at the systemic level through the detection of the soluble form of CD163 in human sera. Collectively, this study argues for the pathogenic role of the CD16$^+$CD163$^+$MerTK$^+$pSTAT3$^+$ monocyte-to-macrophage differentiation program and its potential as a target for TB therapy, and promotes the detection of circulating CD163 as a potential biomarker for disease progression and monitoring of treatment efficacy.

***Keywords*:** tuberculosis; STAT3; macrophage activation; monocyte; biomarker; immunomodulation; migration
Cell Research (2015) **25**:1333-1351. doi:10.1038/cr.2015.123; published online 20 October 2015

Introduction

Tuberculosis (TB) is a severe chronic bacterial infection caused by *Mycobacterium tuberculosis* (Mtb). In 2013, TB claimed the life of nearly 1.5 million people, ranking this disease as the second leading cause of death from a single infectious agent (*Global TB report*, WHO, 2014). While TB mortality is slowly declining each year, it is still unacceptably high given that most cases would be curable if better diagnostic tools and correct treatment

*These two authors contributed equally to this work.
#These two authors are co-senior authors.
Correspondence: Isabelle Maridonneau-Parini[a], Olivier Neyrolles[b]
Tel: +33-0-5 61 17 54 58; Fax: + 33-0-5 61 17 59 94
[a]E-mail: Isabelle.Maridonneau-Parini@ipbs.fr
[b]E-mail: Olivier.Neyrolles@ipbs.fr
Received 5 March 2015; revised 31 July 2015; accepted 6 September 2015; published online 20 October 2015

were available to complement existing technologies. A major obstacle is the lack of TB-specific and non-specific immune activation biomarker and bio-signature tools to estimate disease severity, follow drug treatment efficacy, allow prognosis of disease outcome (recovery or relapse) and estimate vaccine protection [1, 2]. As the basis for maintaining the flow of novel biomarker candidates in the product pipeline, fundamental science is necessary to better characterize Mtb interaction with the human host.

Innate immunity plays a key role in host defense against Mtb. Among the immune innate cells involved in this resistance, macrophages are primordial regulators of the balance of pro- and anti-inflammatory immune response in order to ensure the control of bacterial replication and limit the extent of tissue damage following pathogenic insult [3-5]. They perform these roles according to their high degree of phenotypic and functional plasticity in response to environmental clues within tissues, and are classified within a spectrum ranging from pro-inflammatory (M1) to anti-inflammatory (M2) activation programs [6]. Remarkably, Mtb displays a great capacity to influence the differentiation, maturation and activation of macrophages, resulting in an effective evasion of the immune response and increased persistence in the host (for review, see [7-9]). Despite the significant progress in understanding macrophage subversion by Mtb, one aspect that remains poorly studied is how monocytes contribute to the dynamic alteration of the macrophage compartment during ongoing Mtb infection. As monocytes are the precursors of macrophages during inflammation, substantial insights into host defenses are likely to be gained by determining the role of these leukocytes within the TB context. In particular, while there are important clues coming from the zebrafish and mouse models, the human context remains poorly explored [7, 9, 10].

Human blood monocytes are broadly segregated into two major subsets: $CD14^+CD16^-$ (classical) and $CD14^+CD16^+$ (non-classical) monocytes, hereafter designated as $CD16^-$ and $CD16^+$, respectively [11, 12]. Notably, the $CD16^+$ subset accounts for only 10% of the total monocyte population in healthy donors, displaying a unique cell-surface marker expression and cytokine secretion pattern in comparison with its $CD16^-$ counterpart [13, 14]. Indeed, upon stimulation with lipopolysaccharide, $CD16^+$ monocytes isolated from healthy donors secrete higher amounts of pro-inflammatory factors such as tumor necrosis factor-alpha (TNFα), interleukin-1-beta (IL-1) and IL-6, but low amount of the anti-inflammatory mediator IL-10 [13, 15-17]. Other features distinguishing the $CD16^+$ subset are higher antigen processing and presentation, pro-angiogenic behavior and motility [10]. The expansion of $CD16^+$ monocytes is well documented in different types of diseases, mainly deriving from infection or inflammatory conditions [10]. For these reasons, $CD16^+$ monocytes are usually referred to as pro-inflammatory monocytes.

Interestingly, the human monocyte compartment is perturbed in TB patients, as illustrated by the expansion of $CD16^+$ monocytes, which can account for up to 50% of the total monocyte population, and its correlation with the disease severity [18]. This unbalance in the monocyte population is also associated with a higher cell-surface expression for CD14, CD11b, toll-like receptor-2 (TLR2), TLR5, chemokine C-C motif receptor-1 (CCR1), CCR2 and CCR5, as compared with that of healthy individuals [18]. Functional characterization *in vitro* shows that monocytes isolated from TB patients are refractory to efficient dendritic cell (DC) differentiation and deficient in the activation of T lymphocytes, as compared with monocytes from healthy donors [19, 20]. The cause and consequence of this unbalance are still relatively unknown. In addition, it remains to be elucidated whether there is an effect on the ability of monocytes from TB patients to differentiate into macrophages that are capable of controlling the bacilllus' intracellular growth and mount an effective immune response. Indeed, this is a critical functional aspect to assess, along with its prognostic value, in order to determine whether the unbalanced monocyte population is beneficial or detrimental to host defense against TB, and whether this represents a potential bio-signature and target for treatment.

Here we describe that, in the context of TB, human monocytes differentiating towards a macrophage program (referred here to as monocyte-macrophages) are tilted towards an M2-like activation program characterized by the $CD16^+CD163^+MerTK^+pSTAT3^+$ marker phenotype and functional properties such as high protease-dependent motility, pathogen permissivity and immunomodulatory activity. The establishment of this program is mainly dependent on the signal transducer and activator of transcription 3 (STAT3)-dependent signaling pathway, and points towards a detrimental role in host defense against TB. Importantly, our study provides direct correlation of the abundance of $CD16^+CD163^+MerTK^+pSTAT3^+$ cells with TB disease severity in humans and non-human primates (NHPs), and proposes the presence of the soluble form of CD163 (sCD163) in sera as a potential biomarker to monitor disease progression and treatment efficacy.

Results

The secretome of Mtb-infected macrophages favors the

differentiation of human monocytes towards an M2-like activation program

Mtb infection is known to significantly alter monocyte differentiation upon recruitment to pulmonary tissue in mice, alluding to a bystander effect derived from infected resident cells [21]. As the secretome of Mtb-infected macrophages inhibits human monocyte differentiation towards DC program [22], we investigated whether it also alters monocyte-to-macrophage differentiation. To this aim, we devised an *in vitro* model whereby freshly isolated $CD14^+$ monocytes from healthy donors were differentiated towards a macrophage program (M-CSF driven) in the presence of conditioned media from Mtb-infected human macrophages (cmMTB). As a control, we differentiated monocytes using a conditioned media from non-infected macrophages (cmCTR). Unlike treatment with cmCTR, we observed an expansion of the $CD16^+$ population in the cmMTB-treated monocytes (Figure 1A). In addition, we assessed their activation program by flow cytometry in terms of M1 and M2 cell-surface marker expression. Monocytes conditioned with cmMTB differentiated into cells displaying an equivalent or low-

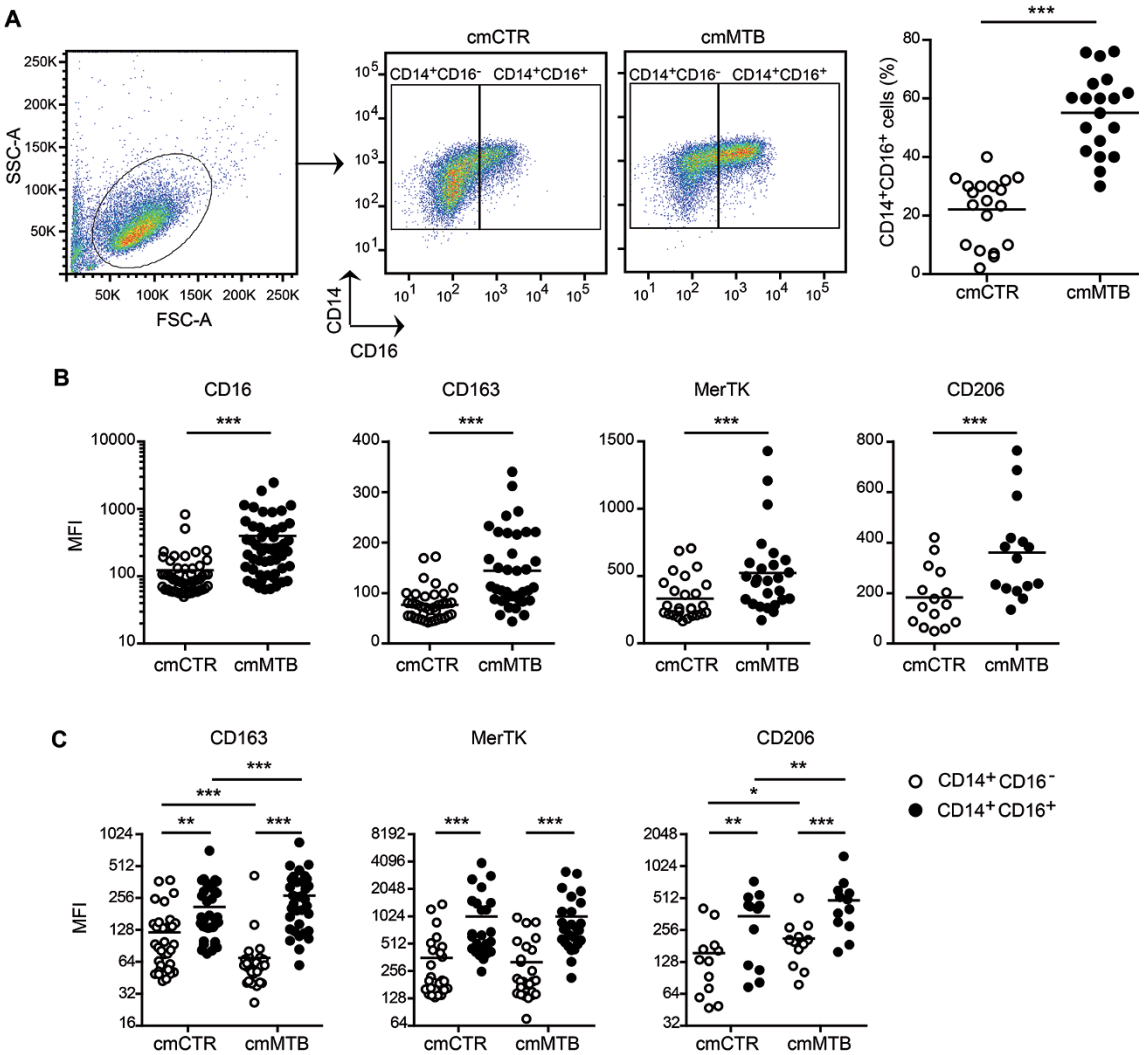

Figure 1 The secretome of Mtb-infected macrophages induces the differentiation of $CD16^+$ monocytes towards an M2-like phenotype. Monocytes were cultured with conditioned media from Mtb-infected (cmMTB, black) or non-infected (cmCTR, white) macrophages. **(A)** Flow cytometry gating strategy of a representative donor and the percentage of $CD14^+CD16^+$ cells. **(B)** Vertical scatter plots showing the median fluorescent intensity (MFI) of cell-surface markers during cmCTR or cmMTB treatment. **(C)** Vertical scatter plots showing the MFI of CD163, MerTK or CD206 in the $CD14^+CD16^-$ (white circles) and $CD14^+CD16^+$ (black circles) cell populations during cmCTR or cmMTB treatment. $^*P < 0.05$, $^{**}P < 0.01$, $^{***}P < 0.001$. Each circle within vertical scatter plots represents a single donor.

er expression of M1 polarization markers (i.e., CD86, HLA-DR, FCAR and Serpine1) compared with cells differentiated in the presence of cmCTR (Supplementary information, Figure S1A-S1B). By contrast, the expression of markers related to M2 macrophage activation, such as CD16, CD163, MerTK, CD206, AMAC1 and CD200R1 [23-27], was upregulated in cmMTB-conditioned cells (Figure 1B, Supplementary information, Figure S1B). Similarly, the expression of CCR2 and CCR5 chemokine receptors was higher in the presence of cmMTB, supporting the acquisition of the M2 program (Supplementary information, Figure S1C) [28, 29]. More precisely, the expression of M2 markers was specifically augmented within $CD16^+$ population compared with the $CD16^-$ counterpart, with a higher increase of CD163 and CD206 upon cmMTB treatment monocytes (Figure 1C).

These results indicate that soluble factors secreted by Mtb-infected macrophages exert bystander effect affecting monocyte differentiation towards an M2-like activation program.

The monocyte activation towards $CD16^+CD163^+MerTK^+$ phenotype is dependent on the IL-10/STAT3 signaling pathway in the TB context

In the presence of M-CSF, IL-10 triggers macrophage M2 activation that promotes tolerance mechanisms, including the resolution of inflammation and tissue repair [28, 30]. Moreover, this cytokine is not only increased in serum and pleural effusion from TB patients compared with healthy donors [31, 32], but also in the lungs of Mtb-infected NHPs [33]. As IL-10 is secreted by Mtb-infected human macrophages [34], we investigated whether it is responsible for the Mtb-derived bystander effect observed in our *in vitro* model. We first examined whether human recombinant IL-10 (recIL-10), in combination with M-CSF, recapitulated the effect of the cmMTB. As expected, the expression of CD206 was not influenced by recIL-10, rather confirming the regulation of this receptor by IL-4/STAT6 axis [35]. By contrast, recIL-10 treatment on monocytes stimulated the expression of M2 markers (i.e., CD16, CD163 and MerTK) compared with control cells, whereas M1 markers were significantly decreased (Supplementary information, Figure S2A). Moreover, when IL-10 was depleted from cmMTB using blocking antibodies (Supplementary information, Figure S2B), we observed impairment in the establishment of the M2 marker signature (except for CD206) (Figure 2A), accompanied by a slight increasing tendency of M1 markers (Supplementary information, Figure S2C), indicating that this cytokine is one of the main soluble factors present in the secretome of Mtb-infected macrophages responsible for the induction of M2-like monocyte-macrophages.

The binding of IL-10 to its receptor leads to the subsequent activation of STAT3, whose role is essential for all known functions of IL-10 [36]. As shown in Figure 2B, short-term exposure of freshly isolated monocytes to cmMTB resulted in STAT3 phosphorylation on tyrosine 705, reflecting its activation. This activation was dependent on the presence of IL-10 since incubation of monocytes with IL-10-depleted cmMTB failed to trigger significant phosphorylation of STAT3 (Figure 2B). Next, we assessed whether STAT3 was crucial for the establishment of M2-like monocyte-macrophages, using a siRNA-mediated gene silencing method [37], or pharmacological inhibition of STAT3 activation with either cucurbitacin I (CCB), which inhibits JAK2 (Janus kinase 2)-dependent phosphorylation of STAT3, or STATTIC, which targets the STAT3-SH2 domain thereby preventing its association with upstream kinases. Both approaches enabled a nearly complete inhibition of STAT3 expression or phosphorylation in human monocyte-macrophages (Supplementary information, Figure S3A-S3C). As expected, inhibition of STAT3 in cmMTB-treated cells reversed the acquisition of the $CD16^+CD163^+MerTK^+$ phenotype, while CD206 or M1 marker expression remained unaffected (Figure 2C and Supplementary information, Figure S3D-S3F).

Altogether, the secretome of Mtb-infected macrophages favors the human monocyte differentiation towards an M2-like activation program, which is mainly but not absolutely dependent (as best indicated by CD206 expression) on the IL-10/STAT3 axis.

The $CD16^+$ monocyte expansion is predisposed towards an M2-like phenotype in patients with active TB

Results obtained through our *in vitro* approach inferred that the reported imbalance in circulating monocyte subsets in TB patients might be associated with a predisposition towards a STAT3-driven M2-like program. To address the physiological relevance of this issue, we analyzed in more detail the activation program of the circulating monocytes in TB patients. We collected peripheral blood from healthy subjects (PB-HS), patients with active (PB-TB) or confirmed latent (PB-LTB) TB (Supplementary information, Table S1), to evaluate the status of the $CD14^+$ monocyte compartment. As previously described [18], we confirmed the higher proportion of $CD16^+$ cells in PB-TB compared with PB-HS, accounting for about 40% of the $CD14^+$ monocytes (Figure 3A, Supplementary information, Figure S4A). Strikingly, the expansion of $CD16^+$ monocytes is non-existent in PB-LTB, indicating that the abundance of these cells is associated with active TB (Figure 3A, Supple-

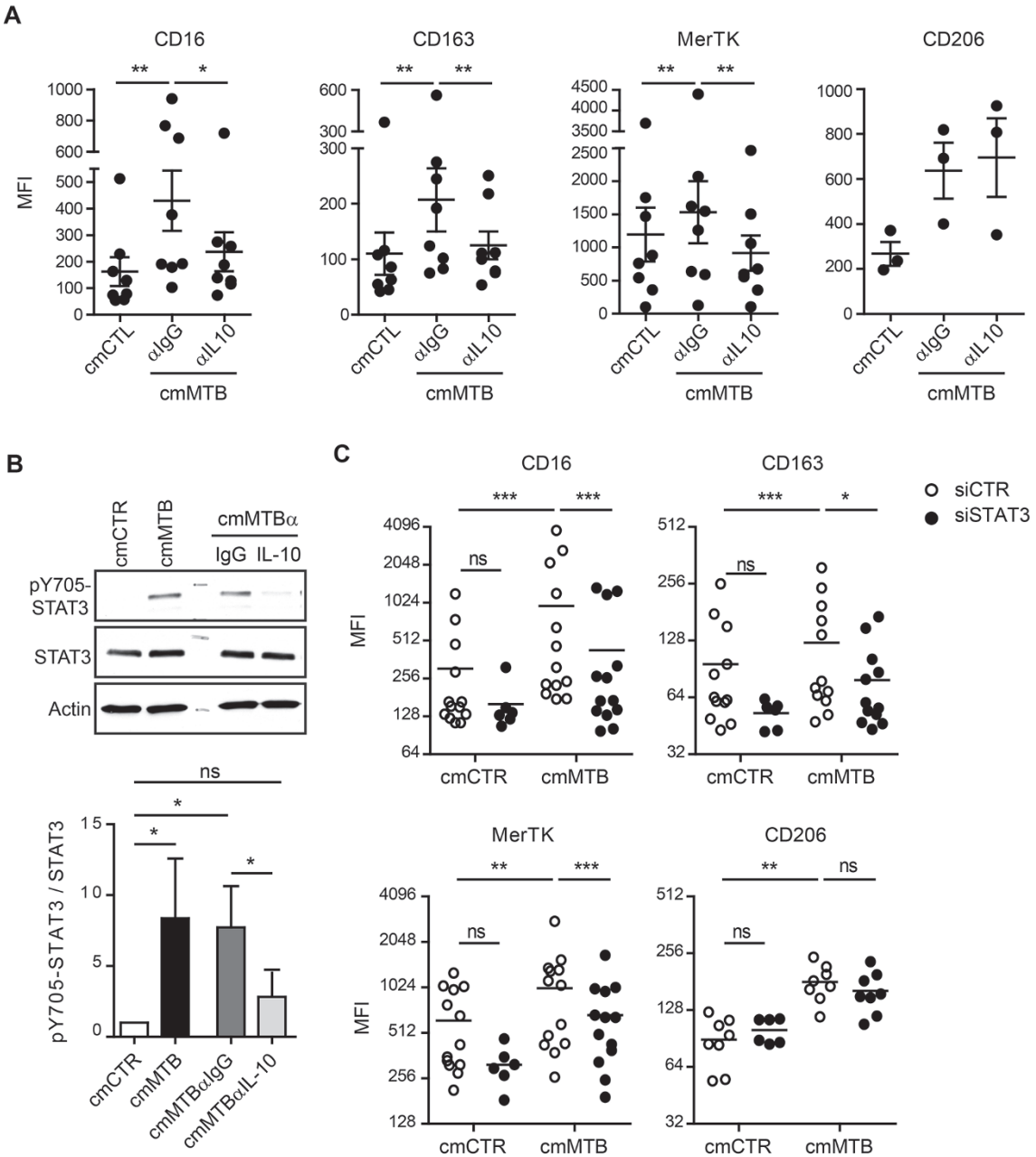

Figure 2 The IL-10/STAT3 pathway drives the predisposition of CD16$^+$ monocytes towards an M2-like phenotype. **(A)** Vertical scatter plots showing the MFI of cell-surface markers in monocytes cultured with IL-10-depleted cmMTB (cmMTBαIL-10) or the mock depletion control (cmMTBαIgG). **(B)** Immunoblot images of pY705-STAT3, STAT3 and actin (upper panel); quantification of pY705-STAT3 versus STAT3 on monocytes after 1 h treatment with cmCTR, cmMTB, cmMTBαIL-10 or cmMTBαIgG (*n* = 6 donors; lower panel). **(C)** Vertical scatter plots showing the MFI of cell-surface markers in monocytes transfected with STAT3 (siSTAT3-black) or non-targeting control (siCTR-white) siRNAs, and conditioned with cmCTR or cmMTB. **P* < 0.05, ***P* < 0.01, ****P* < 0.001. Each circle within vertical scatter plots represents a single donor.

mentary information, Figure S4B). While we failed to correlate the enhanced level of CD16 expression with the M2-like phenotype characterized in our *in vitro* model (Supplementary information, Figure S4B), freshly isolated monocytes from TB patients displayed higher level of phosphorylated STAT3 compared with their counterparts from healthy subjects (HS), as measured by western blot analysis (Figure 3B). Using a flow cytometry-based

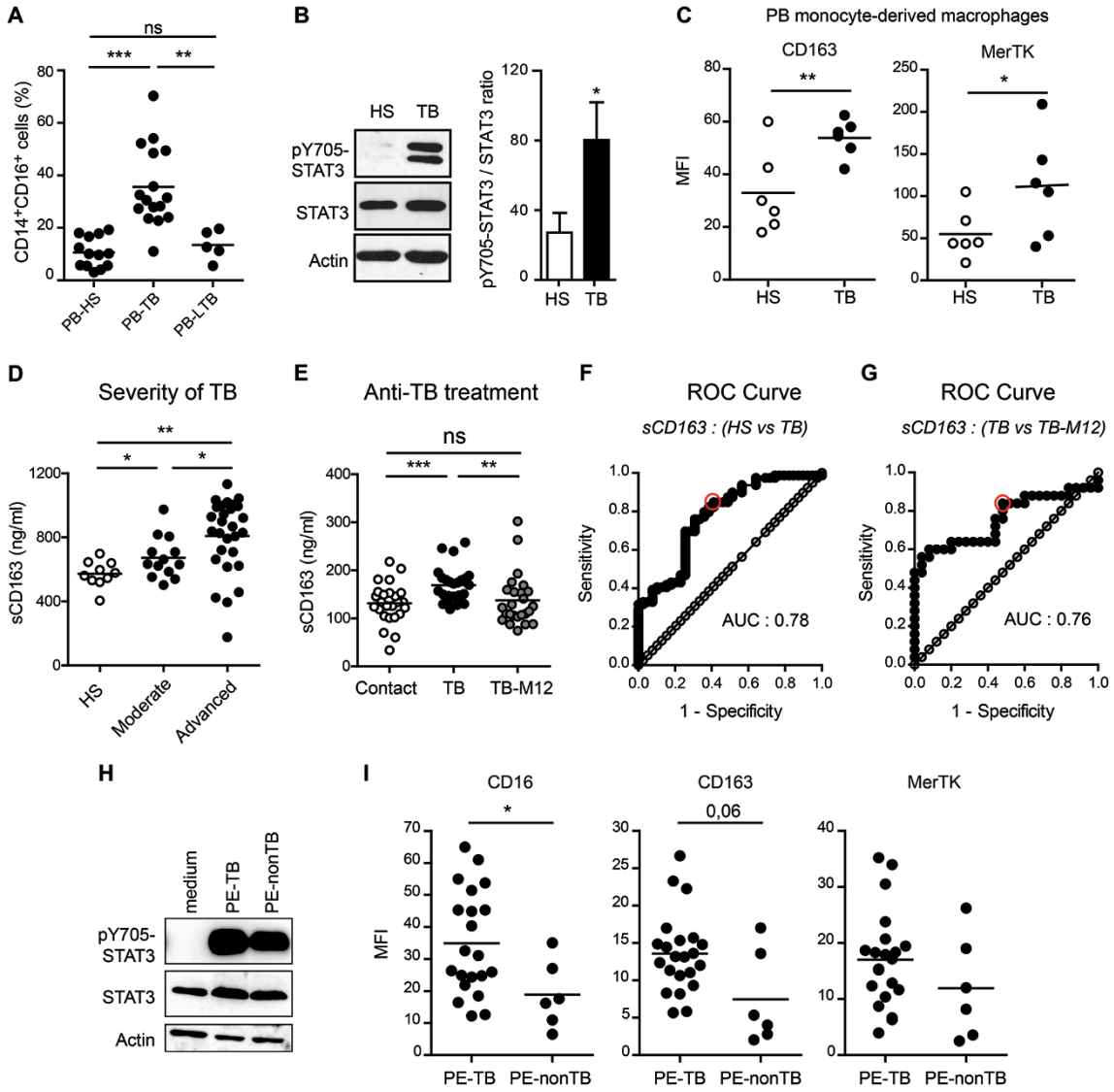

Figure 3 The CD16$^+$ monocyte expansion is predisposed towards an M2-like phenotype in patients with active TB. **(A)** Vertical scatter plots showing the percentage of CD14$^+$CD16$^+$ cells in the peripheral blood of healthy subjects (PB-HS), TB patients (PB-TB) or subjects with latent TB (PB-LTB). **(B)** Immunoblot images of pY705-STAT3, STAT3 and actin (left), and quantification of pY705-STAT3 versus STAT3 (right) on monocytes from healthy subjects (HS) or TB patients (TB) (n = 5 donors). **(C)** Vertical scatter plots showing the MFI of cell-surface markers in HS or TB monocyte-derived macrophages differentiated *in vitro* for 7 days. **(D)** Analysis of soluble form of CD163 (sCD163) level in sera of TB patients according to disease severity, as compared with HS. **(E)** Vertical scatter plots showing the serum level of sCD163 in TB patients before and 12 months after start of treatment (TB-M12), as compared with contact donors. **(F)** ROC (receiver operating characteristic) curve of sCD163 concentration in TB patients compared with HS. **(G)** ROC curve of sCD163 concentration in TB patients before versus after treatment (TB versus TB-M12). The red circle represents the optimal cut point. **(H)** Monocytes from HS were treated with pleural effusion (PE) from TB (PE-TB) or non-TB (PE-nonTB) patients, or culture medium. Representative images of western blot illustrating the expression of pY^{705}-STAT3, STAT3 and actin (n = 3). **(I)** Vertical scatter plots showing the MFI of CD16, CD163 or MerTK on CD14$^+$ monocytes present in PE-TB or PE-nonTB from patients. *P < 0.05; **P < 0.01; ***P < 0.001. Each circle within vertical scatter plots represents a single donor. AUC, area under the curve.

approach, we found that CD14$^+$CD16$^+$ can be differentiated into two sub-populations according to the phosphorylation status of STAT3 (CD14$^+$CD16$^+$pSTAT3$^-$ and CD14$^+$CD16$^+$pSTAT3$^+$). In TB patients, the percentage of CD14$^+$CD16$^+$pSTAT3$^+$ is significantly increased (37.5% ± 11.2%) compared with control donors (13.2% ± 6.1%,

$P < 0.01$, $n = 6$). Moreover, when differentiated *in vitro* with M-CSF, blood monocytes from TB patients exhibited a $CD163^{hi}MerTK^{hi}HLA\text{-}DR^{lo}CD86^{lo}$ macrophage phenotype (Figure 3C, Supplementary information, Figure S4C). Together, these results point out a predisposition of the human monocyte compartment towards an M2-like program in the TB context.

We previously reported that the expansion of peripheral $CD16^+$ monocytes correlates with disease severity of TB patients [18]. To further characterize the activation program of this expanded cell population, we then assessed the M2-like phenotype of circulating monocytes isolated from patients with different clinical parameters to distinguish TB severity (Supplementary information, Table S2). Unlike CD163, we observed that the cell-surface expression of MerTK is significantly augmented in the case of patients with an advanced degree of the disease and accentuated within the $CD16^+$ monocyte subset (Supplementary information, Figure S4D-S4E). Given that membrane-bound CD163 and MerTK receptors are subjected to inflammation-driven shedding [38, 39], we hypothesized that chronic infection with Mtb may also lead to the shedding of these receptors from the surface of circulating monocytes, and thus increase the expression of soluble CD163 (sCD163) and MerTK (MerTK ectodomain: sMer) in the serum of TB patients. Aside from a single report describing the circulating sCD163 as a predictive value for patient survival [40], there is virtually no information about this scavenger receptor and MerTK in the TB context. We thus evaluated the sera from pulmonary TB patients and revealed a progressively increasing trend in the levels of sCD163, particularly striking in cases with an advanced degree of the disease (Figure 3D). Next, to examine whether the soluble expression of this receptor is related to the presence of bacilli, we measured sCD163 serum concentration in TB patients before and after treatment (Supplementary information, Table S3). Noticeably, the TB-induced expression of sCD163 is decreased significantly after treatment (Figure 3E). This was further supported by receiver operating characteristic (ROC) curve analysis showing the relationship between the sensitivity and specificity at any cutoff values for sCD163 (Figure 3F and 3G). For TB patients in relation to HS, the area under the ROC curve (AUC) value for sCD163 was 0.78 (± 0.04) with a 95% confidence interval (CI) of 0.69 to 0.86 ($P < 0.0001$), with an optimal cut point yielding a sensitivity of 84.8% and specificity of 58.9% (Figure 3F). For TB patients, before treatment in relation to the same cases after 12-month treatment (TB-M12), the AUC value for sCD163 was 0.76 (± 0.07) with a CI of 0.61 to 0.90 ($P < 0.001$), with an optimal cut point providing a sensitivity of 84% and specificity of 52% (Figure 3G). In the case for sMer, however, we found no evidence supporting its shedding in TB (Supplementary information, Figure S4F-S4I). These results indicate that altered serum levels of sCD163 might be of potential use as a non-invasive biomarker for pulmonary TB disease progression and monitoring of treatment efficacy.

To further explore the association between Mtb infection and the alteration of the human monocyte compartment, we obtained pleural effusion fluids from TB patients (PE-TB) and other non-TB-related infectious diseases (PE-nonTB; Supplementary information, Table S1). As PE-TB is the most common form of extrapulmonary TB, we tested its capacity to influence the activation program of freshly isolated monocytes from HS, and noticed that both PE-TB and PE-nonTB were able to induce a rapid phosphorylation of STAT3 (Figure 3H). Importantly, when assessing the $CD14^+$ population isolated directly from PE-TB, we observed that these cells tend to display a higher acquisition of the $CD16^+CD163^+MerTK^+$ phenotype in comparison with their counterparts from PE-nonTB (Figure 3I), suggesting that an Mtb-derived microenvironment influences the human monocyte compartment via STAT3.

The abundance of the $CD16^+CD163^+MerTK^+pSTAT3^+$ cell population correlates with pathology severity in non-human primate pulmonary TB

Pulmonary granuloma formation is a hallmark of TB, and the activation program of monocyte-macrophages is thought to play an important role in this process [41]. Therefore, we further investigated whether the M2-like $CD16^+CD163^+MerTK^+$ cell population is present in pulmonary granulomas of Mtb-infected NHPs. The NHP tissue samples were derived from BCG (Bacillus Calmette-Guérin) vaccinated and unvaccinated Mtb-infected rhesus macaques, exhibiting different degrees of lung pathology that was in general inversely correlated with time to end point (survival; Supplementary information, Figure S5A). Immunohistochemical analyses revealed that macrophage infiltration ($CD68^+$) increased according to lung pathology severity (Figure 4A, Supplementary information, Figure S5B); this pattern was also accompanied by increased CD163 expression in tuberculous granulomas in NHPs (Figure 4A, Supplementary information, Figure S5B) [42]. Concomitantly, we observed an elevated expression of CD16 and MerTK in NHP tuberculous granulomas (Figure 4A, Supplementary information, Figure S5B). Notably, the expression of CD163, CD16 and MerTK positively correlated with the severity of lung pathology (Figure 4B). Co-localization analysis within $CD163^+$ macrophages revealed that CD16 and

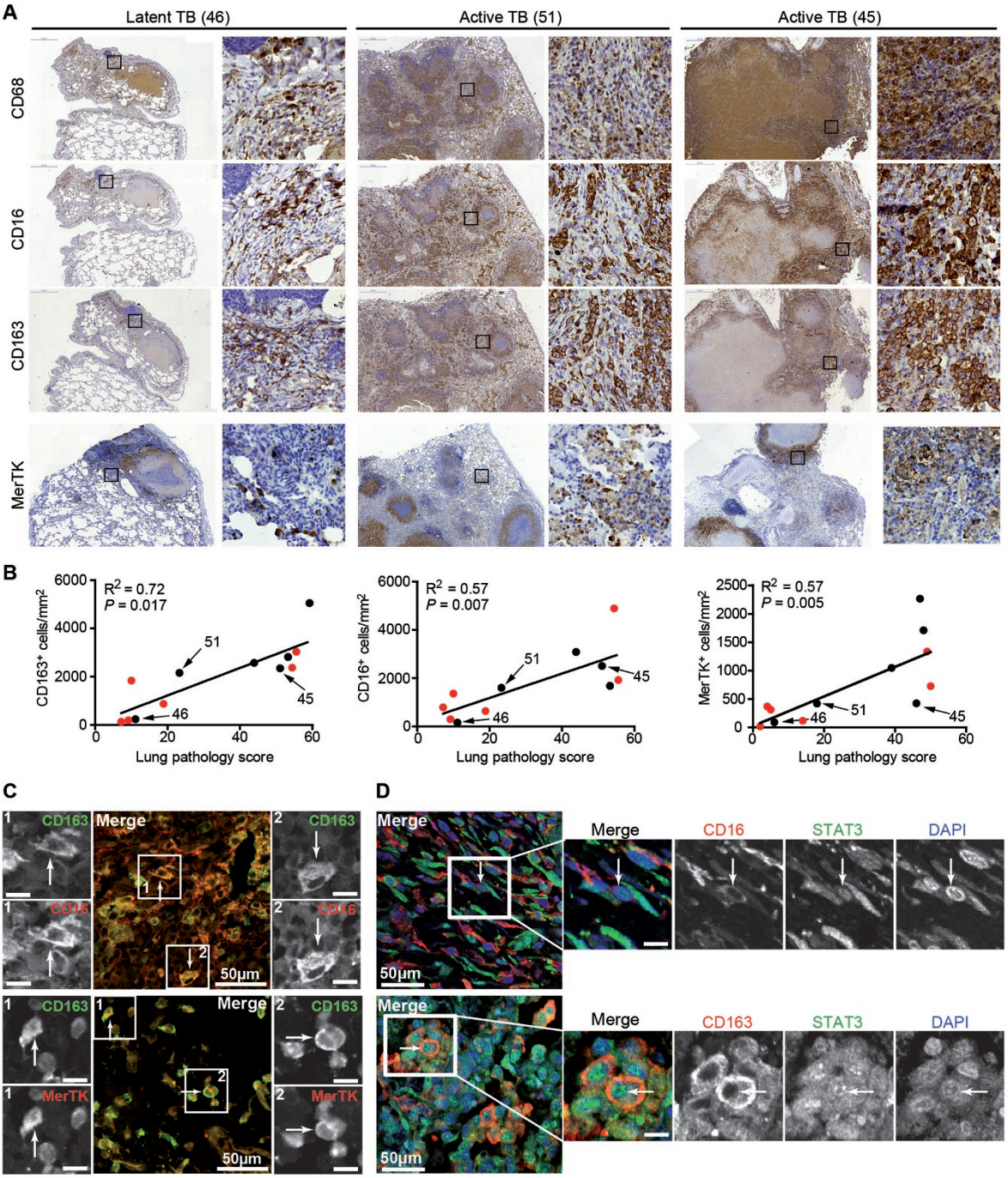

Figure 4 The abundance of the CD16+CD163+MerTK+pSTAT3+ cell population correlates with pathology severity in non-human primate (NHP) pulmonary TB. **(A)** Representative immunohistochemical images demonstrate expression and distribution of CD68, CD16, CD163 and MerTK in lung granulomas from non-vaccinated Mtb-infected NHPs exhibiting different severity of pulmonary TB. NHP numbers refer to Supplementary information, Table S6. **(B)** Correlation analysis between the number of CD16+, CD163+ or MerTK+ cells in lung tissue and lung pathology score in BCG-vaccinated (red circles) or -non-vaccinated (black circles) Mtb-infected NHPs. **(C**, **D)** Immunohistochemistry stainings of lung biopsies from NHP n°51 (intermediate). **(C)** Upper panel: co-localization of CD163 (green; Alexa-488) and CD16 (red; Alexa-555) in lung tissue; lower panel: co-localization of CD163 (green; Alexa-488) and MerTK (red; Alexa-555) in lung tissue. White arrows indicate double-positive cells that are magnified in 1 and 2 (inset scale bar = 10 μm). **(D)** Upper panel: nuclear localization of STAT3 (green; Alexa-488) in CD16 (red; Alexa-555)-positive cells in lung tissue; lower panel: nuclear localization of STAT3 (green; Alexa-488) in CD163 (red; Alexa-555)-positive cells in lung tissue. White arrows indicate CD16- or CD163-positive cells with STAT3 translocated in the nucleus stained with DAPI (blue; inset scale bar = 10 μm).

MerTK were co-expressed in this population (Figure 4C). Even though phosphorylated STAT3 could not be assessed in the NHP samples due to technical reasons, we did observe accumulation of STAT3 in the nuclear area of $CD163^+$ and $CD16^+$ cell populations, indicating that this transcription factor is activated in these leukocytes (Figure 4D).

Collectively, these results suggest that the environment created during pulmonary TB is capable to modulating macrophage activation into an M2-like program, which becomes accentuated according to disease severity.

The $CD16^+CD163^+MerTK^+pSTAT3^+$ monocyte-macrophages display an efficient ability to migrate in dense matrices

To determine whether the expansion of the M2-like monocyte-macrophages is beneficial or detrimental to host defense against TB, we investigated functional consequences of this activation program. Studies performed in zebrafish model showed that the environment induced by mycobacterial infection stimulates the recruitment of highly motile macrophages in a matrix metalloproteases (MMP)-dependent manner, which is known to enhance the pathogenesis [43, 44]. On the basis of these observations, we investigated whether cmMTB influences human monocyte-macrophages migration in different 3D environments that mimic tissues [45]. Cell migration was first analyzed in dense Matrigel in which protease-mediated matrix digestion is mandatory for macrophage infiltration, in contrast to protease-independent migration in porous fibrillar collagen I matrices [45]. In Matrigel, when cmMTB was used as chemoattractant, the migration of human monocyte-macrophages into this matrix was enhanced and the distance covered by the cells was increased (Figure 5A, Supplementary information, Figure S6A). Similar results were obtained using another

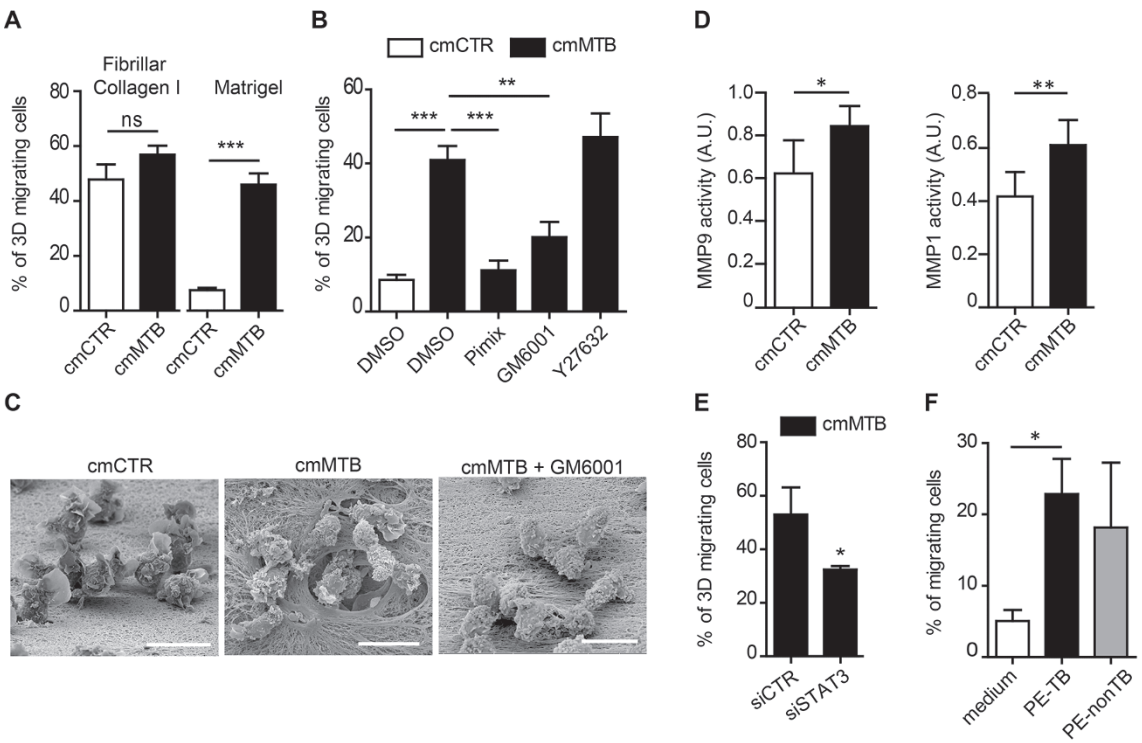

Figure 5 The $CD16^+CD163^+MerTK^+pSTAT3^+$ monocyte-macrophages display a strong ability to migrate in dense matrices. **(A)** Human monocytes were seeded on the top of fibrillar collagen I or Matrigel matrices, and allowed to migrate in response to cmCTR (white) or cmMTB (black). Quantification of the percentage of migrating cells (n = 7 donors). **(B)** Effect of protease (Pimix), matrix metalloprotease (GM6001), Rho-associated kinase (Y27632) inhibitors or DMSO on cell migration in Matrigel (n = 9 donors). **(C)** Representative scanning electron microscopy images showing the matrix remodeling activity of cells on Matrigel (n = 3 donors, scale bar = 10 μm). **(D)** Quantification of gelatin zymogram gels for MMP9 (left) and MMP1 (right) activities (n > 4 donors). **(E)** Monocytes transfected with SMARTpool targeting STAT3 (siSTAT3) or non-targeting control siRNAs (siCTR) were seeded on Matrigel and allowed to migrate in response to cmMTB (n = 3 donors). **(F)** Monocytes from HS were seeded on Matrigel and allowed to migrate in response to PE-TB, PE-nonTB or culture medium (n = 3 donors). Results are expressed as mean ± SEM. *P < 0.05, **P < 0.01, ***P < 0.001.

dense matrix such as gelled collagen I, strengthening the use of protease activity during cmMTB-induced migration (Supplementary information, Figure S6B). In contrast, cells infiltrated the porous fibrillar collagen I matrix efficiently regardless of the provided chemoattractant, cmMTB or cmCTR (Figure 5A). We showed in the past that macrophage 3D migration in dense matrices depends on both protease activity and the tyrosine kinase Hck, but not the ROCK kinase pathway [37, 45-47]. In line with these previous findings, both a cocktail of protease inhibitors (Pimix) and the broad-spectrum MMP inhibitor GM6001 abrogated the cmMTB-enhanced migration into Matrigel (Figure 5B). Moreover, this process was also partially inhibited by siRNA-mediated silencing of Hck in these cells (Supplementary information, Figure S6C). As expected, the use of a ROCK kinase inhibitor (Y27632) had no effect on the cmMTB-enhanced motility in Matrigel (Figure 5B). To further support the role of MMP in the monocyte-macrophage migration, we performed scanning electron microscopy. Our observations revealed that in response to cmMTB, cells profoundly remodeled the matrix compared with those treated with the cmCTR or the MMP inhibitor (Figure 5C). Interestingly, while MMP1 and MMP9 activities were increased in the culture medium of cmMTB-treated cells (Figure 5D), the MMP2 activity was unchanged (Supplementary information, Figure S6D), alluding to the selectivity of MMPs in cmMTB-enhanced motility.

Next, we investigated which soluble factor in cmMTB induces monocyte 3D migration in Matrigel. In zebrafish and mouse models, the chemokine C-C motif ligand-2 (CCL2)-dependent recruitment of $CCR2^+$ macrophages plays a critical role in the mycobacterial pathogenesis [44, 48]. Here we found that migration in Matrigel is mainly based on chemoattraction mediated by recombinant CCL5 but not CCL2 or CCL4 (Supplementary information, Figure S6E). Despite the fact that the expression of CCR2 and CCR5 was enhanced by cmMTB (Supplementary information, Figure S1C), and that their different chemokine ligands are strongly secreted by Mtb-infected macrophages [29, 34], the depletion of CCL2, CCL4 and CCL5 from cmMTB did not significantly alter their migration properties (Supplementary information, Figure S6F). Since the activation program of macrophages modulates their 3D migration capacities [49], we hypothesized that the enhanced cell motility in response to cmMTB might result from the acquisition of the M2-like phenotype. To explore this possibility, we first conditioned freshly isolated monocytes with cmCTR or cmMTB, and then tested their migration capacity in Matrigel without a specific chemoattractant. Compared with cmCTR-treated cells, those treated with cmMTB

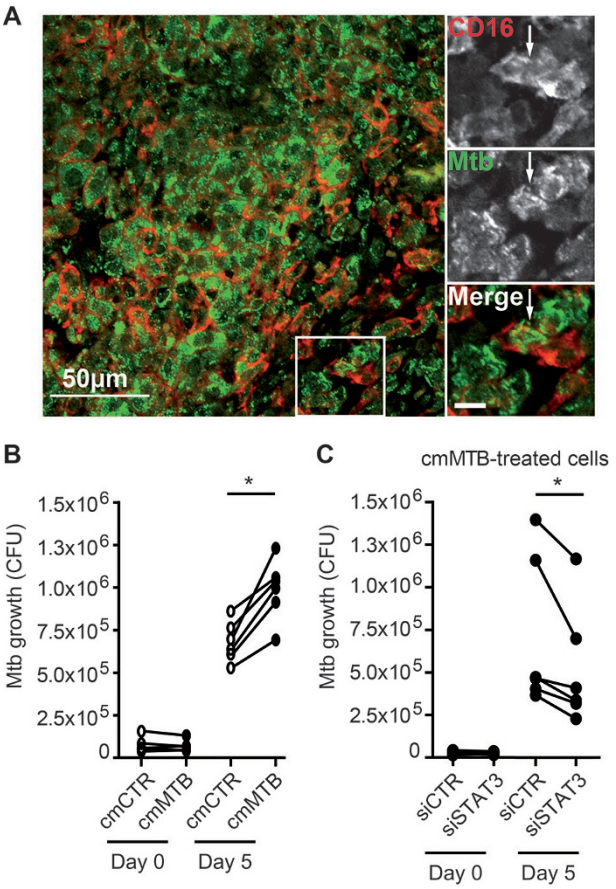

Figure 6 The $CD16^+CD163^+MerTK^+pSTAT3^+$ monocyte-macrophages are associated with a permissive phenotype to Mtb infection. **(A)** Representative confocal microscopy images of $CD16^+$ cells (red, Alexa-555) in lung granulomas from NHP N°51 infected by Mtb (green, Alexa-488). White arrow indicates $CD16^+$ cells containing Mtb bacilli (inset, scale bar = 10 μm). **(B)** Monocytes conditioned with cmCTR (white circles) or cmMTB (black circles) were infected with Mtb. On day 0 and day 5 after infection, the intracellular growth of Mtb was scored by colony-forming unit (CFU) assay. **(C)** Monocytes transfected with SMARTpool targeting STAT3 (siSTAT3) or non-targeting control siRNAs (siCTR) were conditioned with cmMTB, and then infected with Mtb. The CFU scoring was measured on day 0 and day 5 after infection. Results are expressed as before-and-after plot; $*P < 0.05$.

efficiently infiltrated and remodeled Matrigel (Supplementary information, Figure S6G), indicating that acquisition of the M2-like phenotype is sufficient to enhance 3D migration regardless of a chemoattractant gradient. Furthermore, the Mtb-derived bystander effect can be mimicked when monocytes were conditioned with recIL-10 (Supplementary information, Figure S6H-S6I). Consistently, when STAT3 expression was inhibited in

these cells, or IL-10 was depleted from cmMTB, the protease-dependent migratory capacity of conditioned cells was impaired (Figure 5E, Supplementary information, Figure S6I).

Since the monocyte-macrophages characterized by the $CD16^+CD163^+MerTK^+$ signature are abundant in the TB pleural cavity, we assessed whether PE-TB fluid activates the motility of these cells. For these experiments, we used non-TB pleural fluid (PE-nonTB) as a positive control since it is known to activate STAT3 and serve a chemoattractant [50]. As illustrated in Figure 5F, freshly isolated monocytes from healthy donors displayed a greater capacity to infiltrate Matrigel when PE-TB and PE-nonTB were used as chemoattractants.

Taken together, our analysis shows that the acquisition of $CD16^+CD163^+MerTK^+pSTAT3^+$ activation program via the IL-10/STAT3 axis triggers MMP-dependent motility and allows human monocytes to penetrate and remodel dense tissue environments.

The $CD16^+CD163^+MerTK^+pSTAT3^+$ monocyte-macrophages are associated with a permissive phenotype to Mtb infection

The migration of mononuclear phagocytes towards infectious sites is essential for effective control and clearance of bacteria [51]. First, we observed that, among other cell types, $CD16^+$ cells in NHP tuberculous granulomas contained bacilli, implying that these leukocytes can be infected *in vivo* (Figure 6A). Since M2 macrophages are associated with pathogen permissivity [3], we evaluated the ability of monocytes conditioned with cmMTB or cmCTR, and then infected with Mtb, to control bacilli growth. CFU scoring at four hours post infection (p.i.) revealed that there was no difference in the bacterial loads present in cmCTR- and cmMTB-treated cells, suggesting that soluble factors present in cmMTB do not affect the recognition and uptake of the bacilli (Figure 6B). However, cmMTB-treated cells were significantly more permissive to Mtb growth than cmCTR-treated cells, as illustrated at day 5 p.i. (Figure 6B). Inhibition of STAT3 by siRNA-mediated gene silencing in cmMTB-treated cells reversed their pathogen-permissive phenotype (Figure 6C, Supplementary information, Figure S7A). Similar results were obtained by an alternative approach using the pharmacological inhibition of STAT3 activation with STATTIC (Supplementary information, Figure S7B).

Collectively, these results show that the $CD16^+CD163^+MerTK^+pSTAT3^+$ activation program acquisition renders human monocyte-macrophages more susceptible to intracellular bacterial growth.

The $CD16^+CD163^+MerTK^+pSTAT3^+$ monocyte-macrophages display immuno-modulatory properties

M2 macrophages programmed with IL-10, TGFβ or glucocorticoids are known as "deactivators" of the immune response [28]. Among the features that distinguish these cells is the low production of pro-inflammatory cytokines (e.g., TNFα and IL-12), contrasting with high expression of anti-inflammatory mediators (e.g., IL-10, TGFβ and Gas6) [28, 39]. We first assessed the ability of cmMTB-conditioned cells to engage production of inflammatory signals in response to killed Mtb, in order to discriminate the well-described suppressive effects using live Mtb [4]. Our results indicate that, compared with cells treated with cmCTR, those conditioned with cmMTB expressed less pro-inflammatory genes, such as *TNF, IL12A* and *CCL1* (Supplementary information, Figure S8A). The reduced secretion of TNFα was confirmed in the supernatant of cmMTB-treated cells (Supplementary information, Figure S8B). Strikingly, a weaker expression of *IL-10* was observed in contrast to the elevated level of *GAS6* and *PROS1*, in cells pretreated with cmMTB (Supplementary information, Figure S8A). Another feature that distinguishes deactivator macrophages is the poor ability to activate T cells [28]. To evaluate this, we first examined the programmed death ligand 1 (PD-L1) expression relative to that of CD86, since an increased PD-L1/CD86 ratio in mononuclear phagocytes is reported to inhibit T cell proliferation and interferon-gamma (IFNγ) production [52]. Noticeably, we found that the PD-L1/CD86 ratio was highly elevated in cmMTB-conditioned cells compared with cmCTR treatment (Figure 7A, Supplementary information, Figure S8C). Stimulation with killed Mtb did not change this unbalanced ratio in cmMTB-conditioned cells (Figure 7A, Supplementary information, Figure S8C). Next, we measured the capacity of cmMTB-conditioned monocyte-macrophages to activate allogeneic human T cells, using peripheral blood lymphocytes labeled with CFSE. Importantly, the cmMTB-conditioned cells displayed a significantly lower capacity to stimulate T cell proliferation and IFNγ production in comparison with cmCTR-treated cells (Figure 7A). While we only observed a tendency towards the reversion of the unbalanced PD-L1/CD86 ratio (Figure 7B), the inhibition of STAT3 phosphorylation with cucurbitacin significantly reverted the cell surface expression of PD-L1 in cmMTB-treated cells and their poor capacity to activate T cells (Figure 7B and Supplementary information, Figure S8D). To validate these observations *in vivo*, we examined whether monocyte-macrophages in TB patients display immunomodulatory properties. As shown in Figure 7C, upon stimulation with killed Mtb, monocytes from PB-TB displayed an elevated PD-L1/CD86 ratio compared with those from PB-HS. In

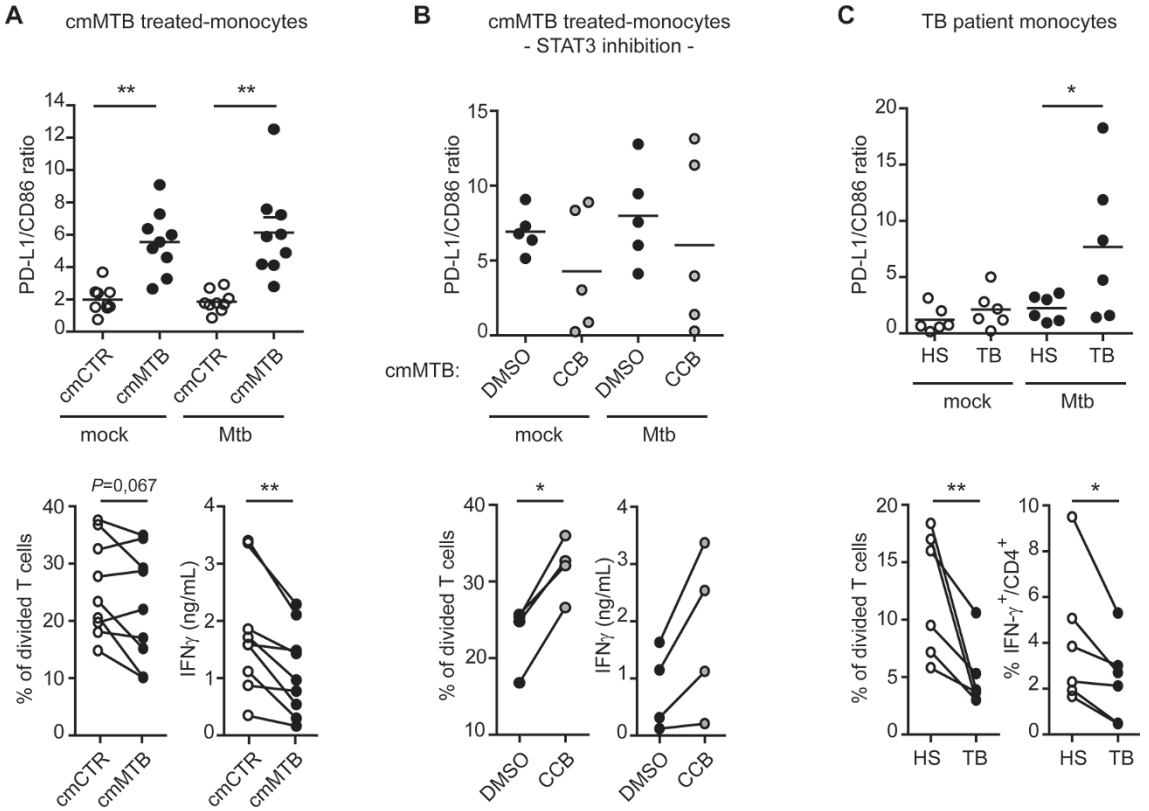

Figure 7 The CD16+CD163+MerTK+pSTAT3+ monocyte-macrophages display immunomodulatory properties. **(A-C)** Monocytes were stimulated with killed Mtb or PBS (mock). Top panels: vertical scatter plots showing the ratio of MFI obtained for PD-L1 and CD86. Results are expressed as mean ± SEM. Bottom panels: allogeneic human T lymphocytes labeled with CFSE were co-cultured with monocytes. Before-and-after plots showing T cell proliferation illustrated as the percentage of CFSE-dividing cells (left) and the production of IFNγ by proliferating T cells quantified by **(A-B)** ELISA in co-culture supernatants or **(C)** flow cytometry (right). **(A)** cmCTR- or cmMTB-conditioned monocytes were stimulated with PFA-killed Mtb or PBS (mock). **(B)** cmMTB conditioning of monocytes was performed in the presence of the STAT3 inhibitor, cucurbitacin I (CCB) or DMSO as control. Cells were then stimulated with PFA-killed Mtb or mock. **(C)** Monocytes from HS or TB patients were stimulated with irradiated Mtb or mock. *P < 0.05; **P < 0.01. Each circle within vertical scatter plots represents a single donor.

addition, PB-TB monocytes exhibited a lower ability to induce T cell proliferation and the production of IFNγ in allogeneic T cells compared with PB-HS monocytes (Figure 7C).

Taken together, these data demonstrate that the acquisition of the CD16+CD163+MerTK+pSTAT3+ activation program is characterized by a (i) low ratio of pro-/anti-inflammatory factor production, (ii) high ratio of PD-L1/CD86 co-stimulatory molecule expression and (iii) poor capacity to activate T cells, which indicates a negative contribution to a dedicated host response against TB.

Discussion

TB mortality is unacceptably high given that most deaths are preventable. The identification of new biomarkers that could reduce the size and duration of clinical trials of new drug candidates and define treatment efficacy, disease activity, cure and relapse, is highly desirable to reduce the impact of TB. Considering that the monocyte compartment is perturbed in TB, we asked whether this shift is beneficial or detrimental to host defense against TB, and whether this could represent a target for treatment. We believe that this study makes four major contributions to the interface between hypothesis-driven basic research and the identification of potential bio-signatures and molecular markers for human disease (Figure 8).

First, we present evidence for how human monocytes are predisposed in the context of TB towards an anti-inflammatory M2-like (CD16+CD163+MerTK+pSTAT3+) macrophage activation program, a process that is mainly

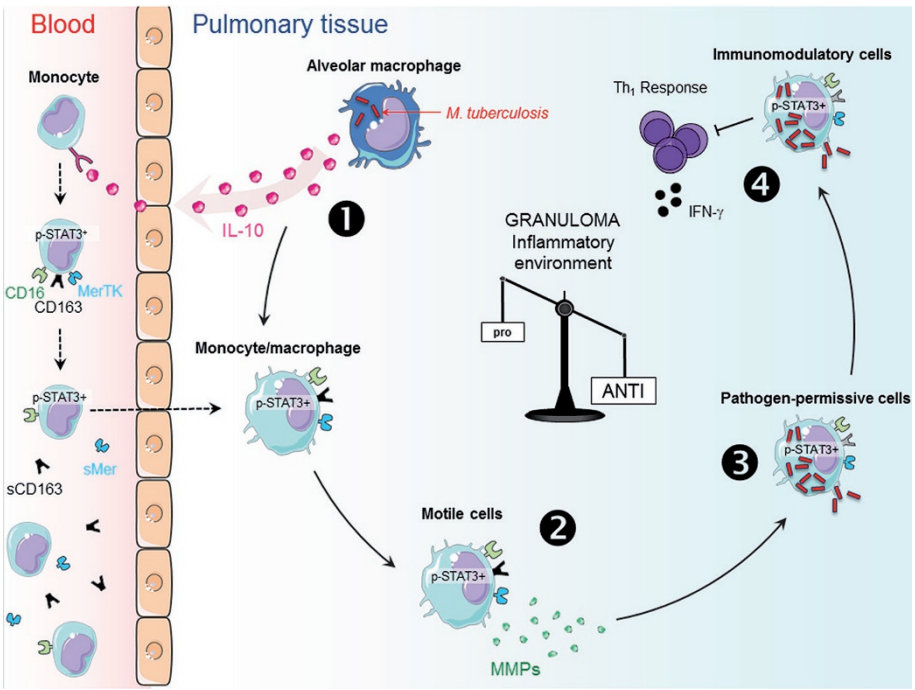

Figure 8 Model illustrating how the environment induced by Mtb infection predisposes human monocyte differentiation towards an M2-like macrophage, altering host defense during infection. Alveolar macrophages are one of the first leukocytes able to recognize and phagocytose Mtb upon entry in the respiratory system. At this site, infected macrophages reshape their microenvironment by secreting many soluble factors including cytokines and chemokines, which for the most part are responsible for the leukocyte infiltration during the earliest stages of infection. However, (1) Mtb has the capacity to modulate the macrophage response and to induce the secretion of anti-inflammatory cytokines, such as IL-10. IL-10, tilts, through a bystander effect, monocytes towards an M2-like macrophage program ($CD16^+CD163^+MerTK^+pSTAT3^+$) in a STAT3-dependent manner. In the blood, CD163 and MerTK receptors are cleaved off, and concentration of their soluble form correlates positively with disease severity. The $CD16^+CD163^+MerTK^+pSTAT3^+$ phenotype acquisition is accompanied by (2) an enhanced protease-dependent motility through matrix metalloprotease activity (e.g., MMP-1), which allows extracellular matrix remodeling, and hypothetically, trans-tissular migration. This phenotype acquisition also renders (3) monocyte-macrophages permissive to Mtb intracellular growth, and (4) immunomodulatory in terms of their reduced ability to secrete pro-inflammatory cytokines (e.g., low TNFα) and activate the T-helper 1 (Th1) response via co-stimulatory signaling (e.g., high ratio PD-L1/CD86). Collectively, the Mtb-derived bystander activation of STAT3 in monocytes predisposes their differentiation program towards a macrophage population that ultimately shifts the microenvironment (e.g., tuberculous granulomas) in favor of microbial resilience in the host.

dependent on the IL-10/STAT3 signaling pathway. This phenotype can also be obtained *in vitro* using the secretome of Mtb-infected macrophages. We provide a new set of markers to characterize this M2-like activation program in terms of hallmark cell-surface markers (i.e., $CD16^+$, $CD163^+$ and $MerTK^+$), the transcription factor STAT3, cytokine content (e.g., $TNF\alpha^{low}$), chemokines receptors (i.e., $CCR2^{high}$ and $CCR5^{high}$), co-stimulatory molecules (i.e., $PD\text{-}L1^{high}$ and $CD86^{low}$) and MMP (i.e., $MMP1^{high}$ and $MMP9^{high}$). Interestingly, we also detected CD206 expression as part of the described M2-like phenotype, which was independent of the IL-10/STAT3 axis. Since CD206 is known to be dependent of STAT6 signaling [53], it is probable that alternative signals (e.g., IL-2, IL-15 and IFNα), which are part of the secretome of Mtb-infected macrophages, are partially responsible for the establishment of this M2-like phenotype. Nevertheless, in our *in vitro* model, the blocking of IL-10 in the Mtb-derived conditioned media seems to be sufficient to impair STAT3 activation and the establishment of M2-like phenotype. This is in line with the fact that IL-10 is considered to be an important clinical biomarker of disease progression [54], increased levels for this cytokine are reported in both the blood [31, 55] and in the bronchoalveolar lavage of active TB patients [56], and in the tuberculous granuloma context in NHP model [57]. The fact that we observed elevated levels of activated STAT3 in monocyte-macrophages in both TB patients and in the

NHP tuberculous granuloma context, suggests that overactive production of IL-10 may be responsible. It remains to be seen whether activation of STAT3 by other signals, such as IL-6 or IL-27, generates a similar activation program with critical consequences for TB pathogenesis and other chronic inflammatory diseases.

Second, mainly based on our *in vitro* approach, we characterized key functional properties for the human $CD16^+CD163^+MerTK^+pSTAT3^+$ monocyte-macrophages. To begin, we provided evidence that these cells display an enhanced capacity to migrate through dense matrices in an MMP-dependent manner contrasting with our previous observations that 3D migration in dense matrices rather involves cathepsins [45, 47, 58, 59]. While we cannot exclude that chemokines present in cmMTB could be involved in the migration capacity of $CD16^+CD163^+MerTK^+pSTAT3^+$ monocyte-macrophages, we showed that STAT3-dependent acquisition of the M2-like phenotype is essential for the enhanced motility and extracellular matrix remodeling activity in these cells. This process is accompanied by MMP1 and MMP9 activity that may contribute to lung tissue damage and TB pathogenesis, as suggested by the formation of protease-mediated tunnels in 3D matrices [47, 60, 61], by a study demonstrating that MMP1 is increased during Mtb infection and is responsible for lung immunopathology [62], and by other reports evidencing the role of MMP9 in the recruitment of macrophages, granuloma maturation and bacterial dissemination [44]. This is an exciting finding given that, in the zebrafish and mouse models, mycobacteria infection recruits highly motile macrophages as a tool for bacterial dissemination [44, 48]. Another functional characteristic described in this study is the permissive nature of $CD16^+CD163^+MerTK^+pSTAT3^+$ cells to handle Mtb intracellular growth. To our knowledge, our study is the first to demonstrate that abrogation of STAT3 in monocyte-macrophages restores the control of Mtb intracellular growth. Actually, STAT3 has been shown to block phagolysosome fusion, induction of autophagy, and optimal release of nitric oxide and reactive oxygen species [63]. However, the regulation of these microbicidal activities by STAT3 has yet to be explored for TB [63]. This is in line with the antagonistic effect of IL-10 on microbicidal activities of Mtb-infected macrophages, such as phagosome-lysosome fusion [63, 64], and IFNγ-induced production of oxygen and nitrogen species [65]. Likewise, mice overexpressing IL-10 specifically in the macrophage compartment present susceptibility to Mtb infection due to macrophages displaying an exaggerated M2-like activation program associated with a high pulmonary bacterial load [66]. In parallel, we also demonstrate that $CD16^+CD163^+MerTK^+pSTAT3^+$ monocyte-macrophages display an immunomodulatory functional capacity. Besides the diminished pro-inflammatory cytokine response, $CD16^+CD163^+MerTK^+pSTAT3^+$ cells also display a high PD-L1 to CD86 ratio and tolerant capacity to control T cell activation. This is in accordance with different reports showing that STAT3 is a key anti-inflammatory mediator that inhibits important pro-inflammatory processes [36, 63]. For instance, mice deficient for the IL-27 receptor (a STAT3 activator) exhibited an uncontrolled production of pro-inflammatory cytokines, elevated levels of IFNγ-producing T cells, enhanced macrophage effector functions and reduced bacterial loads, in response to Mtb infection. Yet, these animals eventually succumb to uncontrolled immunopathology [67]. In a reciprocal case, a mouse with targeted deletion in the myeloid compartment for the suppressor of cytokine signaling-3 (SOCS3), which is known to inhibit STAT3, showed increased susceptibility to Mtb infection [68]. On the basis of these functional observations, our study provides an original biological context to further understand at the molecular level how STAT3 activity grants protease-dependent migration capacity and inhibits antimycobacterial effector mechanisms, consequently opening up new venues to investigate how it might contribute to tissue remodeling, pathogen dissemination and immunomodulation. Beyond the immunomodulatory capacity (Figure 7C), it remains to be shown whether this IL-10/STAT3-dependent functional program is truly established during the expansion of $CD16^+CD163^+MerTK^+pSTAT3^+$ monocyte-macrophages in patients with active TB.

The third major contribution from this study concerns the critical correlation of the abundance of $CD16^+CD163^+MerTK^+pSTAT3^+$ monocyte-macrophages with the severity of TB disease in the human and NHP contexts. Recent studies by Zizzo *et al*. [25, 69] suggested a strict correlation between systemic lupus erythematosus (SLE) disease severity and the activation of an M2-like macrophage characterized by CD163 and MerTK expression during the monocyte-to-macrophage differentiation. Expanding upon our previous observation that the monocyte compartment becomes perturbed in TB patients [18], we now report that the $CD163^+MerTK^+pSTAT3^+$ signature accompanies the expansion of the $CD16^+$ monocytes. As these results contrast with the pro-inflammatory phenotype of $CD16^+$ monocytes in healthy donors [13, 15-17], we infer that all $CD16^+$ monocytes are not created in a similar manner, and thus the CD16 expression in monocyte-macrophages cannot be extrapolated to indicate a pro- or anti-inflammatory nature. Their final differentiation program might result as a consequence of the microenvironment shaped in health and disease pro-

gression contexts. In agreement with a recent description of $CD163^+$ macrophages during the onset of tuberculous pleurisy [70], we show that this M2-like macrophage is particularly enriched within the $CD14^+CD16^+$ cell population isolated from the pleural cavity of TB patients. Considering that the $CD16^+$ population expansion displays an M2-like phenotype in the pleural cavity from TB patients, and that TB pleural effusion activates STAT3 phosphorylation in monocytes from healthy donors and stimulates their protease-dependent migration, we infer that the environmental signals within Mtb infection sites perpetuate the $CD16^+CD163^+MerTK^+pSTAT3^+$ activation program and possibly also serve as chemoattractant. At the tissue level, although there are key reports integrating the concept of macrophage activation within tuberculous granulomas [41, 42], to our knowledge this is the first study to identify the $CD16^+CD163^+MerTK^+$ macrophage activation program along with the co-localization of activated STAT3. Beyond the detection of CD163, we now provide a novel marker signature composed of CD16, MerTK and activated STAT3, which could be helpful to identify the anti-inflammatory and immunomodulatory macrophage program in the progression of TB disease. Based on the known inhibitory role for IL-10 in the formation of protective mature granulomas during Mtb infection [63, 71], the presence of these cells may represent a cellular indicator of granulomas that foment the expansion and dissemination of disease [41, 44]. Indeed, human $CD16^+CD163^+MerTK^+pSTAT3^+$ macrophages meet the criteria for the formation of pathogenic granulomas mainly described in the zebrafish model: secretion of MMPs involved in granuloma formation (i.e., MMP1 and MMP9), high protease-dependent motility, pathogen permissiveness and immunomodulatory capacity to regulate a pro-inflammatory environment [44]. For example, the monocyte predisposition towards M2-like macrophage program alters protective granuloma formation during *Schistosoma mansoni* infection, which indicates a general process contributing to granulomatous diseases [72]. On the basis of these observations, we propose that the unbalanced monocyte compartment in TB is predisposed to differentiate towards the anti-inflammatory M2-like macrophages as a continuously failed attempt by the host to limit immunopathology, whose abundance is directly related to the severity of TB disease, ultimately contributing to the establishment of chronic infection.

The last major contribution of this study is the identification of soluble form of CD163 as a potential biomarker to monitor, in combination with actual and next to be discovered biomarkers, TB disease progression and anti-TB treatment efficacy. Unlike the $CD14^+CD16^+$ cell population found in the pleural cavity, we failed to detect CD163 as part of the cell-surface marker signature in circulating monocytes in TB patients. This was an intriguing observation as circulating monocytes from TB patients still displayed high level of phosphorylated STAT3 and immunomodulatory potential in terms of high PD-L1 to CD86 expression ratio along with a poor capacity to activate allogeneic T cells. The detection of sCD163 in TB patients reconciled these observations, as monocytes are the only circulating cell population known to express CD163 and MerTK [38, 73]. Indeed, the plasma level of these soluble receptors correlated with TB disease severity in patients, and upon anti-TB treatment, it significantly decreased to the plasma concentration level obtained from contact individuals. As sCD163 shows optimal sensitivity and specificity according to the ROC analysis provided in the TB context, we thus propose this soluble receptor, in combination with actual diagnosis tools and next to be discovered molecules, as a potential biomarker to evaluate disease progression and predict drug treatment outcome. In a second step, these results need to be confirmed in a larger cohort of individuals from different genetic background. Indeed, there is only one study that correlated the plasma concentration of sCD163 to the survival of verified TB patients [40]. However, there has been no confirmation of these results ever since, and more importantly, there is no actual evaluation available on the effect of anti-TB drugs on sCD163 levels until now. Interestingly, sCD163 is considered as a valuable marker of the activation of an M2-like monocyte-macrophage program and biomarkers of disease activity in SLE [25, 40], alluding to a critical biological significance for the presence of this soluble receptor as immune response biomarkers in TB disease.

In conclusion, our study provides a novel cellular context, along with identification of molecules and pathways, which may fuel new research venues concerning monocyte-macrophages in the TB context. Newly recommended guidelines for the nomenclature of the macrophage activation process are based on three principles: source of macrophages, definition of activators and a consensus collection of markers to describe macrophage activation [23]. On the basis of these guidelines, the human $CD16^+CD163^+MerTK^+pSTAT3^+$ activation program described in this study within the TB context is reasonably related to the proposed "M(IL-10)" nomenclature. However, in a pathological context, multiple signals can activate STAT3-dependent signaling pathways (e.g., IL-6, IL-23 and IL-27) [36, 63]. Consequently, it remains to be determined whether they activate STAT3 in a similar fashion as IL-10 to specifically establish the TB-associated $CD16^+CD163^+MerTK^+pSTAT3^+$ phenotype and functional profile reported in this study; if so, the no-

menclature "M(STAT3)" would be a way to subsume the phenotype and functions of cells belonging to STAT3-dependent activation program(s). Interestingly, global biomarker studies are sometimes criticized as being non-hypothesis driven [2]. We believe that the functional characterization of this M(IL-10)-like program, and its critical *in vivo* assessment in TB patients and NHP tuberculous granulomas, adds a significant pathological context to the biomarker potential of sCD163. Finally, since immune impairment is usually observed in patients with chronic infections, and given that the STAT3 activity grants a tolerance capacity to the myeloid compartment [36], we estimate that short-term blockade of STAT3 within the monocyte-to-macrophage differentiation program has the potential to modulate mechanisms of disease tolerance and restore the antimicrobial immunity. STAT3 inhibitors, currently assessed in phase I clinical trials for their antitumor effects [74, 75], might be particularly useful in patients with TB meningitis, for example, who fail to control mycobacterial proliferation because of intrinsic exacerbation of immune suppression, and in which dexamethasone treatment has deleterious effects [76].

Materials and Methods

Human and NHP samples

Studies involving human samples from healthy donors and TB patients, and samples from NHPs were performed in accordance to guidelines approved by all indicated Ethical committees; see Supplementary information, Data S1.

Preparation of human monocytes and monocyte-derived macrophages

Monocytes from healthy donors and from TB patients were isolated by CD14 positive magnetic labeling and differentiated into macrophages as previously described [18, 37, 45]; see Supplementary information, Data S1.

Preparation of conditioned media and monocyte treatment

The cmMTB medium was prepared from *Mtb*-infected monocyte-derived macrophages at a multiplicity of infection (MOI) of three bacteria per cell, in RPMI 1640 (Gibco) containing 10% FBS (Sigma-Aldrich). The cmCTR medium was obtained from uninfected macrophages. After overnight incubation at 37 °C, culture media were collected, sterilized by filtration and aliquots were stored at −80 °C. For conditioning, human $CD14^+$ sorted monocytes were allowed to adhere for 1 h on glass coverslips in the absence of serum and then cultured for 3 days with 50% dilution of cmMTB or cmCTR containing M-CSF (Peprotech, 10 ng/ml) and 10% FBS. Cell surface expression of macrophage activation markers (Supplementary information, Table S4), and bacterial intracellular growth, were measured using standard procedures detailed in Supplementary information, Data S1.

3D migration assays

3D migration assays were performed as previously described [45]. Briefly, fibrillar collagen I, gelled collagen I or Matrigel was polymerized in transwell inserts and used immediately. Cells were seeded on top of matrices, the lower chamber of each insert was filled with a 50% dilution of cmMTB or cmCTR in complete medium or with complete medium supplemented with recIL-10. Cell migration into fibrillar collagen I was quantified after 24 h, whereas the migration in dense matrices (Matrigel or gelled collagen I) was quantified after 72 h. The percentage of cell migration was obtained as the ratio of cells within the matrix to the total number of counted cells as described [45].

Assessment of the inflammatory cytokine response and activation of T cells

Total RNAs were reverse transcribed and amplified as detailed in Supplementary information, Data S1. Primers for qPCR are listed in Supplementary information, Table S5. The mRNA content was normalized to the metastatic lymph node protein 51 (MLN51) mRNA and quantified using the ΔΔCt method. Secreted TNFα and IL-10 were measured by ELISA. Activation of allogeneic T cells was evaluated in mixed lymphocyte reactions including cell proliferation by flow cytometry and secreted IFNγ analysis by ELISA or flow cytometry.

Plasma biomarker measurements

Concentrations of soluble sCD163 and sMer (R&D system DuoSet) were assessed in cryopreserved human serum samples maintained at −80 °C, according to the manufacturer's instruction. For sCD163 analysis, the serum was diluted at 1/10, and for sMer at 1/2, in PBS.

Statistical analyses

One-tailed paired or unpaired *t*-test was applied on data sets with a normal distribution, whereas one-tailed Mann-Whitney (unpaired test) or Wilcoxon (matched-paired test) tests were used otherwise. $P < 0.05$ was considered statistically significant. Correlations were evaluated using the Pearson's test. For biomarker measurements, a ROC curve was generated. The AUC value and 95% CI were calculated to determine the specificity and sensitivity of TB infection. All statistical analyses were performed using GraphPad Prism 6.0 (GraphPad Software Inc., USA).

Acknowledgments

This work was supported by the CNRS, the European Union (ERA-NET/ERASysBio grant TB-HOST-NET, and FP7 grants HEALTH-F4-2011-282095-TARKINAID and 241745 NEWTB-VAC), the French National Research Agency (ANR grants 2010-01301 MigreFlame and ANR-12-BSV3-0002 B-TB) and by Fondation pour la Recherche Médicale (FRM, DEQ 20110421312). CL (FDT 20130928326) and GL-V (SPF20110421334) acknowledge support from FRM; AB acknowledges support from ANR-12-BSV3-0002. FAWV acknowledges support from Aeras (Rockville, MD, USA) for the NHP study. This work was also partially supported by the PICT 2012-0221 and PICT 2011-0572 grants given by the Agencia Nacional de Promoción Científica y Tecnológica, Argentina.

References

1 Wallis RS, Kim P, Cole S, *et al*. Tuberculosis biomarkers discovery: developments, needs, and challenges. *Lancet Infect Dis* 2013; **13**:362-372.
2 Kaufmann SH, Parida SK. Tuberculosis in Africa: learning from pathogenesis for biomarker identification. *Cell Host Microbe* 2008; **4**:219-228.
3 Benoit M, Desnues B, Mege JL. Macrophage polarization in bacterial infections. *J Immunol* 2008; **181**:3733-3739.
4 Lugo-Villarino G, Verollet C, Maridonneau-Parini I, Neyrolles O. Macrophage polarization: convergence point targeted by *mycobacterium tuberculosis* and HIV. *Front Immunol* 2011; **2**:43.
5 Flynn JL, Chan J, Lin PL. Macrophages and control of granulomatous inflammation in tuberculosis. *Mucosal Immunol* 2011; **4**:271-278.
6 Martinez FO, Gordon S. The M1 and M2 paradigm of macrophage activation: time for reassessment. *F1000prime Rep* 2014; **6**:13.
7 Lugo-Villarino G, Neyrolles O. Manipulation of the mononuclear phagocyte system by *Mycobacterium tuberculosis*. *Cold Spring Harb Perspect Med* 2014; 4: a018549.
8 O'Garra A, Redford PS, McNab FW, *et al*. The immune response in tuberculosis. *Annu Rev Immunol* 2013; **31**:475-527.
9 Cambier CJ, Falkow S, Ramakrishnan L. Host evasion and exploitation schemes of *Mycobacterium tuberculosis*. *Cell* 2014; **159**:1497-1509.
10 Wong KL, Yeap WH, Tai JJ, *et al*. The three human monocyte subsets: implications for health and disease. *Immunol Res* 2012; **53**:41-57.
11 Robbins CS, Swirski FK. The multiple roles of monocyte subsets in steady state and inflammation. *Cell Mol Life Sci* 2010; **67**:2685-2693.
12 Ziegler-Heitbrock L. The CD14+ CD16+ blood monocytes: their role in infection and inflammation. *J Leukoc Biol* 2007; **81**:584-592.
13 Frankenberger M, Sternsdorf T, Pechumer H, Pforte A, Ziegler-Heitbrock HW. Differential cytokine expression in human blood monocyte subpopulations: a polymerase chain reaction analysis. *Blood* 1996; **87**:373-377.
14 Frankenberger M, Hofer TP, Marei A, *et al*. Transcript profiling of CD16-positive monocytes reveals a unique molecular fingerprint. *Eur J Immunol* 2012; **42**:957-974.
15 Szaflarska A, Baj-Krzyworzeka M, Siedlar M, *et al*. Antitumor response of CD14+/CD16+ monocyte subpopulation. *Exp Hematol* 2004; **32**:748-755.
16 Belge KU, Dayyani F, Horelt A, *et al*. The proinflammatory CD14+CD16+DR++ monocytes are a major source of TNF. *J Immunol* 2002; **168**:3536-3542.
17 Aguilar-Ruiz SR, Torres-Aguilar H, Gonzalez-Dominguez E, *et al*. Human CD16+ and CD16- monocyte subsets display unique effector properties in inflammatory conditions *in vivo*. *J Leukoc Biol* 2011; **90**:1119-1131.
18 Balboa L, Romero MM, Basile JI, *et al*. Paradoxical role of CD16+CCR2+CCR5+ monocytes in tuberculosis: efficient APC in pleural effusion but also mark disease severity in blood. *J Leukoc Biol* 2011; **90**:69-75.
19 Balboa L, Romero MM, Laborde E, *et al*. Impaired dendritic cell differentiation of CD16-positive monocytes in tuberculosis: role of p38 MAPK. *Eur J Immunol* 2013; **43**:335-347.
20 Tung YC, Ou TT, Tsai WC. Defective *Mycobacterium tuberculosis* antigen presentation by monocytes from tuberculosis patients. *Int J Tuberc Lung Dis* 2013; **17**:1229-1234.
21 Skold M, Behar SM. Tuberculosis triggers a tissue-dependent program of differentiation and acquisition of effector functions by circulating monocytes. *J Immunol* 2008; **181**:6349-6360.
22 Remoli ME, Giacomini E, Petruccioli E, *et al*. Bystander inhibition of dendritic cell differentiation by *Mycobacterium tuberculosis*-induced IL-10. *Immunol Cell Biol* 2011; **89**:437-446.
23 Murray PJ, Allen JE, Biswas SK, *et al*. Macrophage activation and polarization: nomenclature and experimental guidelines. *Immunity* 2014; **41**:14-20.
24 Calzada-Wack JC, Frankenberger M, Ziegler-Heitbrock HW. Interleukin-10 drives human monocytes to CD16 positive macrophages. *J Inflamm* 1996; **46**:78-85.
25 Zizzo G, Hilliard BA, Monestier M, Cohen PL. Efficient clearance of early apoptotic cells by human macrophages requires M2c polarization and MerTK induction. *J Immunol* 2012; **189**:3508-3520.
26 Sironi M, Martinez FO, D'Ambrosio D, *et al*. Differential regulation of chemokine production by Fcgamma receptor engagement in human monocytes: association of CCL1 with a distinct form of M2 monocyte activation (M2b, Type 2). *J Leukoc Biol* 2006; **80**:342-349.
27 Jaguin M, Houlbert N, Fardel O, Lecureur V. Polarization profiles of human M-CSF-generated macrophages and comparison of M1-markers in classically activated macrophages from GM-CSF and M-CSF origin. *Cell Immunol* 2013; **281**:51-61.
28 Mantovani A, Sica A, Sozzani S, *et al*. The chemokine system in diverse forms of macrophage activation and polarization. *Trends Immunol* 2004; **25**:677-686.
29 Verreck FA, de Boer T, Langenberg DM, van der Zanden L, Ottenhoff TH. Phenotypic and functional profiling of human proinflammatory type-1 and anti-inflammatory type-2 macrophages in response to microbial antigens and IFN-gamma- and CD40L-mediated costimulation. *J Leukoc Biol* 2006; **79**:285-293.
30 Verreck FA, de Boer T, Langenberg DM, *et al*. Human IL-23-producing type 1 macrophages promote but IL-10-producing type 2 macrophages subvert immunity to (myco)bacteria. *Proc Natl Acad Sci USA* 2004; **101**:4560-4565.
31 Olobo JO, Geletu M, Demissie A, *et al*. Circulating TNF-alpha, TGF-beta, and IL-10 in tuberculosis patients and healthy contacts. *Scand J Immunol* 2001; **53**:85-91.
32 Liang L, Zhao YL, Yue J, *et al*. Interleukin-10 gene promoter polymorphisms and their protein production in pleural fluid in patients with tuberculosis. *FEMS Immunol Med Microbiol* 2011; **62**:84-90.
33 Roodgar M, Lackner A, Kaushal D, *et al*. Expression levels of 10 candidate genes in lung tissue of vaccinated and TB-infected cynomolgus macaques. *J Med Primatol* 2013; **42**:161-164.
34 Wang C, Peyron P, Mestre O, *et al*. Innate immune response to *Mycobacterium tuberculosis* Beijing and other genotypes. *PLoS One* 2010; **5**:e13594.
35 Szanto A, Balint BL, Nagy ZS, *et al*. STAT6 transcription factor is a facilitator of the nuclear receptor PPARgamma-reg-

ulated gene expression in macrophages and dendritic cells. *Immunity* 2010; **33**:699-712.
36 Lang R. Tuning of macrophage responses by Stat3-inducing cytokines: molecular mechanisms and consequences in infection. *Immunobiology* 2005; **210**:63-76.
37 Troegeler A, Lastrucci C, Duval C, *et al*. An efficient siRNA-mediated gene silencing in primary human monocytes, dendritic cells and macrophages. *Immunol Cell Biol* 2014; **92**:699-708.
38 Fabriek BO, Dijkstra CD, van den Berg TK. The macrophage scavenger receptor CD163. *Immunobiology* 2005; **210**:153-160.
39 Zagorska A, Traves PG, Lew ED, Dransfield I, Lemke G. Diversification of TAM receptor tyrosine kinase function. *Nat Immunol* 2014; **15**:920-928.
40 Knudsen TB, Gustafson P, Kronborg G, *et al*. Predictive value of soluble haemoglobin scavenger receptor CD163 serum levels for survival in verified tuberculosis patients. *Clin Microbiol Infect* 2005; **11**:730-735.
41 Lugo-Villarino G, Hudrisier D, Benard A, Neyrolles O. Emerging trends in the formation and function of tuberculosis granulomas. *Front Immunol* 2012; **3**:405.
42 Mattila JT, Ojo OO, Kepka-Lenhart D, *et al*. Microenvironments in tuberculous granulomas are delineated by distinct populations of macrophage subsets and expression of nitric oxide synthase and arginase isoforms. *J Immunol* 2013; **191**:773-784.
43 Cambier CJ, Takaki KK, Larson RP, *et al*. Mycobacteria manipulate macrophage recruitment through coordinated use of membrane lipids. *Nature* 2014; **505**:218-222.
44 Ramakrishnan L. Revisiting the role of the granuloma in tuberculosis. *Nat Rev Immunol* 2012 **12**:352-366.
45 Van Goethem E, Poincloux R, Gauffre F, Maridonneau-Parini I, Le Cabec V. Matrix architecture dictates three-dimensional migration modes of human macrophages: differential involvement of proteases and podosome-like structures. *J Immunol* 2010 **184**:1049-1061.
46 Cougoule C, Le Cabec V, Poincloux R, *et al*. Three-dimensional migration of macrophages requires Hck for podosome organization and extracellular matrix proteolysis. *Blood* 2010; **115**:1444-1452.
47 Maridonneau-Parini I. Control of macrophage 3D migration: a therapeutic challenge to limit tissue infiltration. *Immunol Rev* 2014; **262**:216-231.
48 Antonelli LR, Gigliotti Rothfuchs A, Goncalves R, *et al*. Intranasal Poly-IC treatment exacerbates tuberculosis in mice through the pulmonary recruitment of a pathogen-permissive monocyte/macrophage population. *J Clin Invest* 2010; **120**:1674-1682.
49 Cougoule C, Van Goethem E, Le Cabec V, *et al*. Blood leukocytes and macrophages of various phenotypes have distinct abilities to form podosomes and to migrate in 3D environments. *Eur J Cell Biol* 2012; **91**:938-949.
50 Yeh HH, Lai WW, Chen HH, Liu HS, Su WC. Autocrine IL-6-induced Stat3 activation contributes to the pathogenesis of lung adenocarcinoma and malignant pleural effusion. *Oncogene* 2006; **25**:4300-4309.
51 Shi C, Pamer EG. Monocyte recruitment during infection and inflammation. *Nat Rev Immunol* 2011; **11**:762-774.
52 Freeman GJ, Long AJ, Iwai Y, *et al*. Engagement of the PD-1 immunoinhibitory receptor by a novel B7 family member leads to negative regulation of lymphocyte activation. *J Exp Med* 2000; **192**:1027-1034.
53 Lawrence T, Natoli G. Transcriptional regulation of macrophage polarization: enabling diversity with identity. *Nat Rev Immunol* 2011; **11**:750-761.
54 Jamil B, Shahid F, Hasan Z, *et al*. Interferon gamma/IL10 ratio defines the disease severity in pulmonary and extra pulmonary tuberculosis. *Tuberculosis (Edinb)* 2007; **87**:279-287.
55 Verbon A, Juffermans N, Van Deventer SJ, *et al*. Serum concentrations of cytokines in patients with active tuberculosis (TB) and after treatment. *Clin Exp Immunol* 1999; **115**:110-113.
56 Bonecini-Almeida MG, Ho JL, Boechat N, *et al*. Down-modulation of lung immune responses by interleukin-10 and transforming growth factor beta (TGF-beta) and analysis of TGF-beta receptors I and II in active tuberculosis. *Infect Immun* 2004; **72**:2628-2634.
57 Souza-Lemos C, de-Campos SN, Teva A, Porrozzi R, Grimaldi G Jr. *In situ* characterization of the granulomatous immune response with time in nonhealing lesional skin of *Leishmania braziliensis*-infected rhesus macaques (*Macaca mulatta*). *Vet Immunol Immunopathol* 2011; **142**:147-155.
58 Wiesner C, Le-Cabec V, El Azzouzi K, Maridonneau-Parini I, Linder S. Podosomes in space: macrophage migration and matrix degradation in 2D and 3D settings. *Cell Adh Migr* 2014; **8**:179-191.
59 Jevnikar Z, Mirkovic B, Fonovic UP, *et al*. Three-dimensional invasion of macrophages is mediated by cysteine cathepsins in protrusive podosomes. *Eur J Immunol* 2012; **42**:3429-3441.
60 Van Goethem E, Guiet R, Balor S, *et al*. Macrophage podosomes go 3D. *Eur J Cell Biol* 2011; **90**:224-236.
61 Guiet R, Van Goethem E, Cougoule C, *et al*. The process of macrophage migration promotes matrix metalloproteinase-independent invasion by tumor cells. *J Immunol* 2011; **187**:3806-3814.
62 Elkington P, Shiomi T, Breen R, *et al*. MMP-1 drives immunopathology in human tuberculosis and transgenic mice. *J Clin Invest* 2011; **121**:1827-1833.
63 Rottenberg ME, Carow B. SOCS3 and STAT3, major controllers of the outcome of infection with *Mycobacterium tuberculosis*. *Semin Immunol* 2014; **26**:518-532.
64 O'Leary S, O'Sullivan MP, Keane J. IL-10 blocks phagosome maturation in *mycobacterium tuberculosis*-infected human macrophages. *Am J Respir Cell Mol Biol* 2011; **45**:172-180.
65 Moore KW, de Waal Malefyt R, Coffman RL, O'Garra A. Interleukin-10 and the interleukin-10 receptor. *Annu Rev Immunol* 2001; **19**:683-765.
66 Schreiber T, Ehlers S, Heitmann L, *et al*. Autocrine IL-10 induces hallmarks of alternative activation in macrophages and suppresses antituberculosis effector mechanisms without compromising T cell immunity. *J Immunol* 2009; **183**:1301-1312.
67 Holscher C, Holscher A, Ruckerl D, *et al*. The IL-27 receptor chain WSX-1 differentially regulates antibacterial immunity and survival during experimental tuberculosis. *J Immunol* 2005; **174**:3534-3544.
68 Carow B, Reuschl AK, Gavier-Widen D, *et al*. Critical and

independent role for SOCS3 in either myeloid or T cells in resistance to *Mycobacterium tuberculosis*. *PLoS Pathog* 2013; **9**:e1003442.
69 Zizzo G, Guerrieri J, Dittman LM, Merri JT, Cohen PL. Circulating levels of soluble MER in lupus reflect M2c activation of monocytes/macrophages, autoantibody specificities and disease activity. *Arthritis Res Ther* 2013; **15**:R212.
70 Tang Y, Hua SC, Qin GX, Xu LJ, Jiang YF. Different subsets of macrophages in patients with new onset tuberculous pleural effusion. *PLoS One* 2014; **9**:e88343.
71 Cyktor JC, Carruthers B, Kominsky RA, *et al*. IL-10 inhibits mature fibrotic granuloma formation during *Mycobacterium tuberculosis* infection. *J Immunol* 2013; **190**:2778-2790.
72 Girgis NM, Gundra UM, Ward LN, *et al*. Ly6Chigh monocytes become alternatively activated macrophages in schistosome granulomas with help from CD4+ cells. *PLoS Pathog* 2014; **10**:e1004080.
73 Graham DK, Dawson TL, Mullaney DL, Snodgrass HR, Earp HS. Cloning and mRNA expression analysis of a novel human protooncogene, c-mer. *Cell Growth Differ* 1994; **5**:647-657.
74 Hayakawa F, Sugimoto K, Harada Y, *et al*. A novel STAT inhibitor, OPB-31121, has a significant antitumor effect on leukemia with STAT-addictive oncokinases. *Blood Cancer J* 2013; **3**:e166.
75 Iwamaru A, Szymanski S, Iwado E, *et al*. A novel inhibitor of the STAT3 pathway induces apoptosis in malignant glioma cells both *in vitro* and *in vivo*. *Oncogene* 2007; **26**:2435-2444.
76 Tobin DM, Roca FJ, Oh SF, *et al*. Host genotype-specific therapies can optimize the inflammatory response to mycobacterial infections. *Cell* 2012; **148**:434-446.

(**Supplementary information** is linked to the online version of the paper on the *Cell Research* website.)